Available online at www.sciencedirect.com
ScienceDirect
Proceedings of the Combustion Institute 33 (2011) 569–576
Proceedings of the Combustion Institute
www.elsevier.com/locate/proci

A study of low-pressure premixed ethylene flame with and without ethanol using photoionization mass spectrometry and modeling

O.P. Korobeinichev [a,*], S.A. Yakimov [a], D.A. Knyazkov [a], T.A. Bolshova [a], A.G. Shmakov [a], Jiuzhong Yang [b], Fei Qi [b]

[a] *Institute of Chemical Kinetics & Combustion, Novosibirsk 630090, Russia*
[b] *National Synchrotron Radiation Laboratory, University of Science and Technology of China, Hefei, Anhui 230029, People's Republic of China*

Available online 25 September 2010

Abstract

In order to investigate the influence of ethanol on the process of forming precursors of polyaromatic hydrocarbons (PAH) and soot in ethylene flame, the measurement results and the 1 D numerical modeling results of the concentration profiles of stable species, as well as of radicals in premixed burner-stabilized flame of the fuel-rich mixture of ethylene/ethanol/oxygen/argon at the pressure of 30 torr are presented and compared. Rich ethylene flame was chosen as the base flame. The measurements were made using molecular beam mass spectrometry with tunable synchrotron photoionization. The concentration of benzene and propargyl radicals, the main PAH precursors, was found to be lower in the flame of the ethylene/ethanol fuel mixture than in the pure ethylene flame. The main reaction pathways leading to benzene formation in ethylene flame containing ethanol and without it were analyzed.

Keywords: Ethylene flame structure; Soot; PAH; Tunable VUV photoionization; Molecular-beam mass spectrometry

1. Introduction

The ability of oxygen-containing compounds (oxygenates) to reduce the CO and NO_x concentrations in the combustion products, as well as to suppress soot formation in hydrocarbon flames has caused great interest for investigating combustion of hydrocarbon and oxygenate mixtures. This is of great practical significance in view of reduction of pollutant emissions, including soot, into air, in order to ensure environmental protection, intensification of the combustion processes in internal combustion engines, in gas turbines and in furnaces, as well as in view of searching for alternative biofuels and their mixtures with oil-produced conventional fuels, to meet the needs of the transport and energy industries. Ethanol, a typical representative of biofuels, currently produced on an industrial scale, is one of the most promising oxygenates.

In a series of studies, the influence of ethanol additives on the combustion of different hydrocarbons, like *n*-heptane [1,2], ethane [3], diesel fuel [4],

* Corresponding author. Address: Institute of Chemical Kinetics & Combustion, Institutskaya st., 3, Novosibirsk, 630090 Russia. Fax: +7 383 3307350.
E-mail address: korobein@kinetics.nsc.ru (O.P. Korobeinichev).

1540-7489/$ - see front matter © 2010 The Combustion Institute. Published by Elsevier Inc. All rights reserved.
doi:10.1016/j.proci.2010.07.066

and propylene [5], was investigated experimentally and with the numerical modeling method. Combustion of ethylene/ethanol mixtures is of great interest for a number of reasons and has been studied in the works [6–9] at the pressure of 1 bar. Ethylene is an important intermediate product, formed in large amounts during oxidation of heavy hydrocarbons. Thus, ethylene flame may be considered as a simplified combustion model for studying combustion of conventional hydrocarbon fuels. In addition, there are several detailed mechanisms of ethylene combustion reactions, well-tested under various conditions, are available in literature [10–12], which may be used for hydrocarbon combustion modeling. The studies [1–9,13] are united by one goal: to develop the mechanism of the influence of oxygenate additives, including ethanol, on formation of soot and PAH, as soot precursors, in different flames by measuring and/or modeling concentration profiles of reactants and intermediate and resulting combustion products. The results obtained in these studies have shown that the effect of ethanol addition can be different depending on the mixing condition.

McNesby et al. [6] measured at the pressure of 1 bar the fluorescence signal for PAH and OH, as well as light absorption by soot in diffusion flames in the counterflows of ethylene and air with ethanol added either to the ethylene flow or to the air flow. The authors have discovered that, when EtOH is added into the ethylene flow, the fluorescence signal gets intensified, indicating that ethanol increases soot formation. The calculations conducted in work [6] taking into account detailed kinetics developed in work [10] have shown that, as ethanol is added to flame, the formation rate of the methyl radical grows, with C_4H_6 formed in the reaction between CH_3 and propargyl C_3H_3. The latter species reacts with C_2 compounds to form benzene C_6H_6. In its turn, the increase of the C_6H_6 concentration leads to the increase in the concentration of PAH and soot. When ethanol was added to the air flow, McNesby and coworkers discovered reduction of soot and its precursors. It was also established with modeling that adding EtOH contributed to the increase in the integral concentration of radicals H, O and OH and to the insignificant increase of the maximum flame temperature. This observation allowed the authors to suppose that reduction of soot and PAH formation was caused in that case by more intense oxidation of soot and PAH, compared to the situation with flame without ethanol addition.

In work [7], the method of laser-induced incandescence was used to measure the volume fraction of soot and the method of laser-induced fluorescence to determine the relative signals of different aromatic species across the premixed rich ethylene/air flames stabilized at the McKenna burner with and without ethanol addition at the pressure of 1 bar. Concentration profiles of individual species were not measured. Thus, ethanol addition was found to reduce the amount of soot and PAH in flame. The results of the conducted numerical 1D modeling using the mechanism of ethylene oxidation and PAH formation [11] have shown that only half of the carbon amount contained in ethanol is consumed with formation of C_2 compounds, which, as noted above, determine formation of aromatic species. Therefore, reduction in the concentration of aromatic species by adding ethanol is caused by the reduction of the fraction of carbon participating in the formation of soot precursors.

McEnally and coworkers [8,9] studied the effect of ethanol on the processes of benzene and soot formation in ethylene and air co-flow diffusion flame at the pressure of 1 bar. The experimentally found increase in the concentration of soot and a number of hydrocarbons C_1–C_{12} was explained as follows. The CH_3 radicals formed in the process of ethanol transformation contribute to the acceleration of the $C_1 + C_2$ addition reactions, resulting in the formation of propargyl radicals, the reaction between which yields benzene, which, in its turn, results in the formation of soot in flame. In addition to the above works, the authors [14] analyzed other experimental data on the effect of ethanol addition to hydrocarbon fuels on soot formation, obtained in a shock tube, a well-stirred reactor and a high-pressure turbulent reactor. The ability of ethanol to reduce soot formation in various experimental devices [15–17] means that the process through which the soot reduction is effected must be common to all of the devices. That common process is chemical kinetics. It can be seen from the above review that ethanol affects on soot formation in various ways, depending on the mixing condition. For better understanding of the chemistry of ethylene combustion with ethanol additives, experimental data on flame structure are required. However, there are no such data in literature. Only experimental and modeling data are available in literature on the concentration profiles for soot, small aromatic species and large PAH, obtained at 1 bar in premixed flame, as well as experimental data on the structure of diffusion flame at 1 bar.

The objective of the given study is to investigate the mechanism of ethanol influence on soot formation in premixed rich ethylene flames by studying the structure of ethylene flames at the pressure of 30 torr with and without ethanol addition, with the help of molecular beam mass spectrometry using synchrotron VUV radiation, as well as computer modeling based on the detailed kinetic mechanism.

2. Experimental

The experiments were conducted in the National Synchrotron Radiation Laboratory,

Hefei, China. Flat laminar premixed flame was stabilized at the horizontally aligned 6 cm diameter McKenna burner under the pressure of 30 torr. A flame sample was extracted from the burning region with a cone-shaped quartz nozzle with 40° aperture angle and 500 μm orifice diameter. A nickel skimmer was used to cut the central part of the molecular beam, which then entered the ionization chamber where it was exposed to synchrotron VUV radiation. Photoions were collected and analyzed by a reflectron time-of-flight mass spectrometer (RTOF-MS). The synchrotron radiation was taken from two beamlines of the 800 MeV electron storage ring: (1) undulator beamline with 1 m Seya–Namioka monochromator equipped with a 1500 grooves/mm grating, energy resolution $E/\Delta E = 1000$, the average photon flux being about 10^{13} photons/s; (2) bend magnet beamline with 1 m Seya–Namioka monochromator equipped with a 1200 grooves/mm grating, energy resolution $E/\Delta E = 500$, average photon flux 5×10^{10} photons/s. A gas filter with inert gas (Ne or Ar) was used to eliminate higher-order harmonic radiation. Photon flux was measured by SXUV-100 silicon photodiode to normalize ion signals. The experimental setup is described in detail in [18]. Two rich ($\varphi = 2.0$) $C_2H_4/O_2/Ar$ (0.28/0.42/0.3) and $C_2H_4/C_2H_5OH/O_2/Ar$ (0.14/0.14/0.42/0.3) flames have been studied. The inlet cold-flow velocity of the combustible mixtures under study v_0 equals 37.33 cm s^{-1}. The mass flow rates for combustible mixtures without and with ethanol addition equal correspondingly 2.35×10^{-3} and 2.19×10^{-3} g $s^{-1}cm^{-2}$. The flame temperature was measured with a 0.076-mm-diameter Pt/Pt–13%Rh thermocouple coated with Y_2O_3-BeO anti-catalytic ceramic [19]. The thermocouple was placed at the distance of 15 mm from the sampling cone orifice. Radiation losses were also taken into account. Ion signal intensities, normalized by the photon flux, were measured and plotted versus: (a) the distance from the burner to the tip of the probe orifice at the constant photon energy (9, 9.5, 10, 10.8, 11.8, 12.3, 13.5, 14.35, and 16.2 eV); and (b) photon energy while the probe was in the middle of the luminous region. The former data provide information about spatial species distribution in flame, while the latter describe the curves of the photoionization effect needed to identify species by their ionization energies. Considering the cooling effect of a molecular beam [20], the errors of IE determination are ±0.05 eV for species with strong signal-to-noise (S/N) ratios and ±0.10 eV for species with weak S/N ratios.

The procedure of mole fraction calculation was described by Cool et al. [21]. Briefly, the ion signal recorded for a flame species i may be written as

$$S_i(T) = CP_i(T)\sigma_i(E)D_i\Phi_P(E)F(k,T,P),$$

where C is the constant of proportionality, T and P_i(T) are the local flame temperature and spatial pressure of species i; σ_i is the photoionization cross-section at the photon energy E; D_i is the mass discrimination factor for species i; Φ_P(E) is the photon flux; $F(k, T, P)$ is the empirical instrumental sampling function that relates the molecular beam molar density in the ionization region to the flame pressure P and the local temperature T; k is the specific heat ratio. The next equation was used to define the major species' mole fractions in flame:

$$X_i(T)/X_i(T_0) = [S_i(T)/S_i(T_0)]/FKT(T,T_0),$$

where X_i is the mole fraction of species i, T_0 refers to the temperature at the burner surface and $FKT(T,T_0)$ is the normalized sampling function

$$FKT(T,T_0) \equiv F(k,T,P)/F(k,T_0,P),$$

which can be constructed by using measurements of signal ratio of argon S_{Ar}(T)/S_{Ar}(T_0). This is suitable for species of entering gases, while the temperature T_F measured at 30 mm from the burner was used for post flame species.

The mole fractions of the other species can be found using the following equation:

$$X_i(T) = S_i(T)[X_j(T)/S_j(T)][\sigma_j(E)/\sigma_i(E)][Dj/D_i].$$

Mass discrimination factors were measured by comparing ion signals in several binary mixtures. Photoionization cross-sections are taken from literature [22–25]. For intermediates with unknown photoionization cross-sections, a method reported by Koizumi is used to estimate the cross-section values [26].

3. Modeling

Kinetic modeling was conducted using the PREMIX code from the CHEMKIN II package. The temperature profile used in calculations was derived from the experimental temperature by lowering it by 100 K [27,28] and shifting 3.5 mm away from the burner surface [29] in order to take into account the thermocouple's temperature disturbance caused by the probe's cooling effects. Such consideration of the temperature profile perturbation has ensured, as shown below, satisfactory agreement between the measurement results and the calculated stable species concentration profiles. The detailed kinetic mechanism consisted of two parts: the base mechanism was developed by Frenklach and co-workers [10] and the ethanol oxidation mechanism was borrowed from Marinov [31]. The reactions selected from the ethanol mechanism were the initial reactions of the molecules themselves such as hydrogen abstraction and unimolecular decomposition, along with reactions of the resulting products that eventually produced

species present in the base mechanism. The thermodynamic data were also combined to provide the required input data. The resultant mechanism contained 121 species and 708 reactions, of which 20 species and 164 reactions were added from the ethanol mechanism. The base mechanism includes pyrolysis and oxidation of C_1 and C_2 species, formation of heavy linear hydrocarbons up to C_6 species, formation of benzene and further reactions leading to formation of pyrene, as well as the oxidation pathways of the aromatic species. The odd-carbon-atom formation of the first aromatic ring occurs by the widely accepted combination of propargyl (C_3H_3) radicals, which are treated as an overall single irreversible step with the rate constant fitted to the experimental species profiles of laminar premixed flames of ethane, ethylene and acetylene against which the model was validated [10,30]. There are 3 versions of this mechanism available: for 90 torr, 1 bar and 10 bar. The first one was used in the present kinetic study. The low-pressure mechanism version was validated against 90 torr acetylene flame. The ethanol mechanism developed by Marinov [31] has been validated against a number of experimental data sets at 40 torr [32] and 1–4.6 bar [31]. These include laminar flame speed data, data from a constant volume bomb and counter-flow twin-flame, ignition delay data behind a reflected shock wave, and ethanol oxidation product profiles from a jet-stirred and turbulent flow reactor. Good agreement between the model and the measurements has been observed for five different experimental systems. This mechanism was developed after a thorough review of the kinetics literature.

4. Results and discussion

Shown in Table S1 in Supplementary Information are the major intermediate products (stable species and radicals) CH_3, C_2H_2, H_2CO, C_3H_3, C_3H_4, C_3H_5, C_2H_6, C_4H_2, C_4H_4, C_4H_6, C_3H_6, C_6H_6, reactants and the resulting combustion products, which have been measured in this work for two flames under study. Table S1 contains the values of photoionization energies, at which measurements were made, and the ionization potentials (IP) measured in this study and taken from literature, as well as maximum concentration values and the distances from the burner surface, at which these values were obtained. In some cases, when the ionization potentials were beyond the range of the photon energy available, these were marked as "not measured". Based on the data presented in the Table, it can be stated that concentrations of most measured intermediate products in these flames have their maxima at the distance of about 5–7 mm from the burner surface. The flame temperature at these distances amounts to about 2200–2300 K. Ethylene/ethanol flame has higher maximum temperature than ethylene flame (2350 and 2000 K, respectively), despite its lower heat of combustion. The difference in temperatures is due to lower heat losses into the burner in the ethylene/ethanol flame, as the velocity of flame propagation for this flame is lower than that of the ethylene flame; hence, with equal mass flow rates of the combustible mixtures, the former flame is at a larger distance from the burner surface than the latter. Comparing the results shown in the Table S1 for the ethylene flame with and without ethanol, a conclusion can be made that maximum concentrations of most intermediate products C_1–C_6, except for oxygenates, formed directly during EtOH oxidation (acetaldehyde, ketene, ethenol and acetone), are lower in the flame containing ethanol than in that containing ethylene only. An important feature is a fact that in the flame containing ethanol, the maximum concentration of benzene, one of the major aromatic soot precursors, is more than 3 times lower than in the flame containing ethylene only. Although we did not make measurements of the concentrations of soot and of aromatic species with the number of benzene rings greater than 1, the very fact that ethanol addition resulted in considerable reduction of benzene concentration testifies to essential slowing down of soot formation processes under the given conditions. This result is in agreement with that previously obtained by Wu et al. [7], whose work was discussed earlier. The latter researchers [7] also observed reduction of PAH and soot concentration in adding ethanol to premixed ethylene and air flame at the pressure of 1 bar. Reduction of the measured concentrations of other intermediate products in the ethylene/ethanol flame, compared to ethylene flame (Table S1) is also significant. For example, maximum concentration of acetylene and of the allyl radicals drops about 1.8 times; that of allene, propyne, diacetylene and vinyl acetylene drops about 2.5–2.7 times, that of formaldehyde and 1.3-butadiene falls 2 times, while the concentration of propargyl, one of the major benzene precursors, decreases 6 times. These facts suggest that the course of chemical reactions in these flames significantly differs. Concentration profiles of the species presented in Table S1 were compared to those calculated for both flames. As seen from Figs. 1 and 2, the detailed kinetic mechanism used well describes the concentration profiles of the reactants (ethylene, oxygen and ethanol) and of the main combustion products (CO_2, H_2O, CO, H_2) in these flames. As far as the intermediate products are concerned, the situation with them is ambiguous: the model predicts concentration profiles for some species quite well, while for a number of species there is essential disagreement between the modeling and experimental data (see figures in Supplementary Information and Figs. 3 and 4). This disagreement

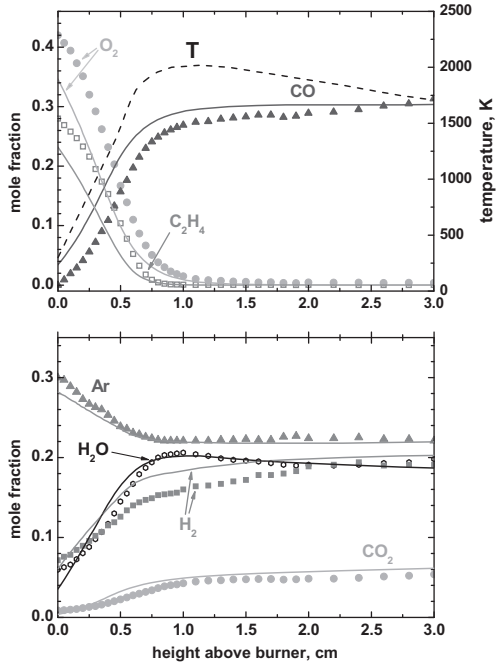

Fig. 1. The measured temperature profile (the dotted line) and the measured (symbols) and calculated (curves) concentration profiles for stable species in the ethylene flame.

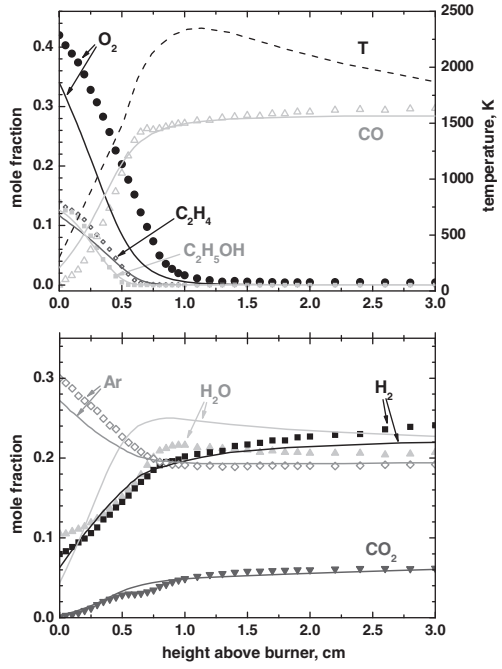

Fig. 2. The measured temperature profile (the dotted line) and the measured (symbols) and calculated (curves) concentration profiles for stable species in the ethylene/ethanol flame.

is mainly of a quantitative nature. To take an example, the model quantitatively describes the concentration profiles for the following intermediate products: C_2H_2, CH_4, H_2, CH_2O, CH_2CO, as well as C_4H_4. Disagreement for CH_3 is a factor of 3–4, for C_3H_3 and C_6H_6 in ethylene flame it is a factor of 2 and 7. However, in ethylene/ethanol flame disagreement for C_3H_3 and for C_6H_6 is a factor of 9 and 10, respectively (See Figures in Supplementary Information and Figs. 3 and 4). Testing the effect of decreasing the temperature profile by 200 K on the calculated profiles of C_6H_6 and C_3H_3 concentrations, the maximum values of which differ from the experimental values by an order of magnitude, has shown this effect to be insignificant. This suggests that disagreement between the calculated and experimental values for these species cannot be accounted for by the incorrect temperature profiles adopted for modeling. Reliability of our experimental data is confirmed by their agreement on the concentration of propargyl and benzene in ethylene flame with the data of [33], obtained in similar conditions. This quantitative disagreement may be caused by imperfection of the mechanism used, which consists, as previously mentioned, of the ethylene combustion mechanism and of the ethanol oxidation mechanism without any additional optimization of the kinetic scheme. We did modeling using the mechanism [30]. The calculation data for the maximum concentrations of C_6H_6 and C_3H_3 are in poor agreement with the experimental data for both flames, especially for ethylene/ethanol flame (disagreement for C_3H_3 reaches a factor of 9). Of special interest is the discrepancy between the predicted propargyl concentration value in ethylene/ethanol flame and the value obtained in the experiment. The calculation showed the propargyl concentration to drop by 22%, while the experimental drop amounted to 85%. This indicates that the mechanism of reduction of soot precursor's concentration by ethanol still needs more work. Another broadly validated mechanism of hydrocarbon combustion, USC-II [34], was also employed for modeling. Comparison of the measured concentration profiles for C_3H_3 and C_6H_6 with those calculated using the USC-II mechanism has indicated that the USC-II mechanism better described experimental data for maximum benzene concentrations and the impact of ethanol on them (Supplementary Fig. S2); however, it is worse in describing the shape of the propargyl concentration profile and its maximum value. In addition, propargyl concentration increases when ethanol is added to ethylene, which is contrary to the experimental result (Fig. S3). To ascertain the reasons for the reduction in the concentrations of PAH and soot precursors under the given conditions, analysis of the benzene formation reaction pathways was made for both flames with the help of KINALC

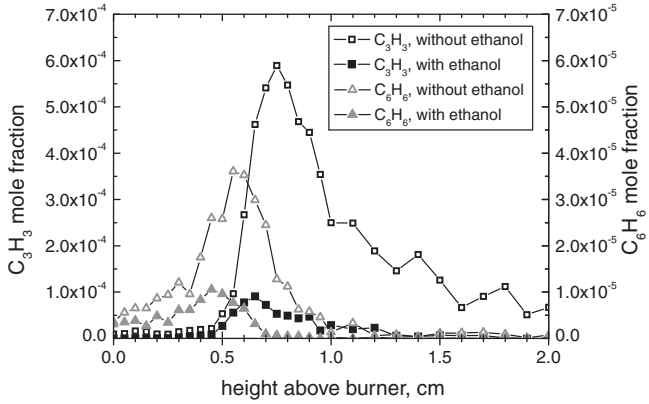

Fig. 3. The measured benzene and propargyl concentration profiles in the ethylene flame (empty symbols) and in the ethylene/ethanol flame (the solid symbols).

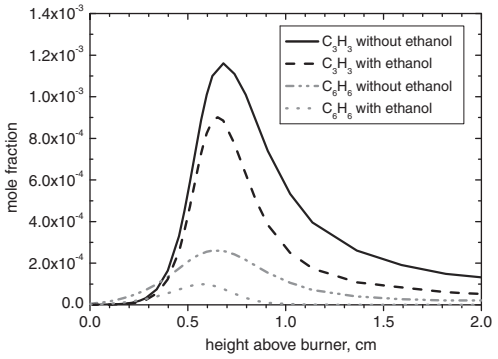

Fig. 4. Calculated benzene and propargyl concentration profiles in the ethylene flame and in the ethylene/ethanol flame.

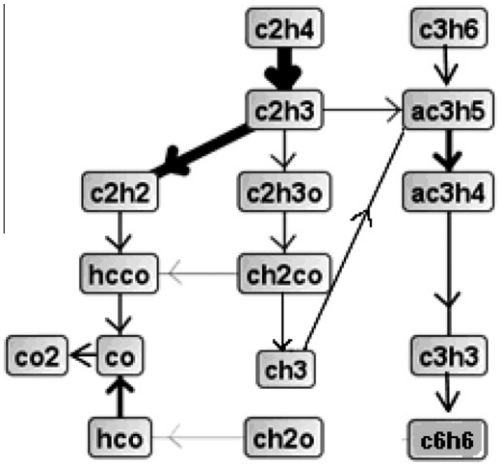

Fig. 5. The scheme of the main transformation pathways (fluxes of element C from species to species) in the ethylene flame.

and FluxViewer codes. The analysis was made for the distances 5.5 and 4.5 mm from the burner surface for the ethylene and ethylene/ethanol flame, respectively. These distances correspond to the maximum rate of benzene production, with the temperature in these points being about 1700 K. Shown in Figs. 5 and 6 are the schemes of the main transformation pathways (the fluxes of element C from species to species) in ethylene flame and in the flame of the mixture C_2H_4+EtOH, respectively. Thickness of arrows in these schemes is proportional to the value of the flux of element C. It is to be noted that, except for the main transformation pathways shown in Figs. 5 and 6, there are numerous not so important pathways, not shown in the schemes.

In the ethylene flame (Fig. 5), ethylene decomposition takes place to form C_2H_3 as a result of a reaction with the H atom: $C_2H_4 + H = C_2H_3 + H_2$. C_2H_3 is mainly consumed along the following three paths: forming acetylene ($C_2H_3(+M) = C_2H_2 + H(+M)$), forming C_2H_3O in the reaction with molecular oxygen ($C_2H_3 + O_2 = C_2H_3O + O$) and forming the allyl radical in the reaction with the methyl radical ($C_2H_3 + CH_3 = aC_3H_5 + H$). The main transformation chain, leading to benzene formation, begins, in accordance with the mechanism used, from the allyl radical, which first transforms into allene (aC_3H_4) according to the reaction $aC_3H_5 + H = aC_3H_4 + H_2$, with a propargyl radical formed from allene according to the reaction with an H atom $aC_3H_4 + H = C_3H_3 + H_2$. Further on, during recombination of the propargyl radicals, benzene is formed: $C_3H_3 + C_3H_3 = C_6H_6$. As seen from Fig. 5, two other transformation pathways for C_2H_3 (except for those forming the allyl radical) do not lead to benzene formation. The maximum rate of benzene formation and its peak concentration are at 1700 K, which is lower than the temperature at which benzene begins to become thermally unstable (>1800 K).

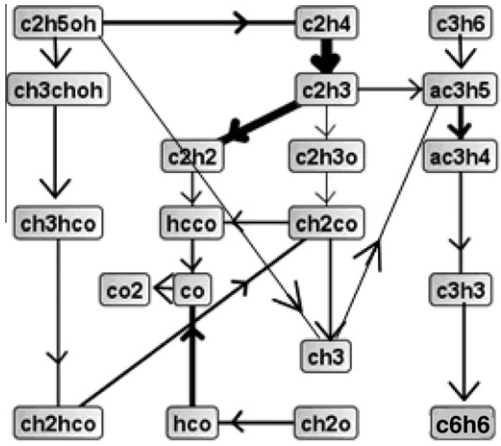

Fig. 6. The scheme of the main transformation pathways (fluxes of element C from species to species) in the ethylene/ethanol flame.

The scheme of ethylene and ethanol transformation pathways in the flame of the fuel mixture C_2H_4 + EtOH (Fig. 6) differs from that considered above mainly by the fact that the ethanol oxidation chain is added to it. It is to be emphasized that the main ethanol consumption (about 56% of the total consumption flux) occurs with ethylene formation (according to the reaction $C_2H_5OH(+M) = C_2H_4 + H_2O(+M)$). Some part of the ethanol is consumed to form a methyl radical according to the reaction $C_2H_5OH(+M) = CH_3 + CH_2OH(+M)$ (16% of the total consumption flux), while some part gives rise to a chain of transformations, resulting in the formation of CH_2CO. The latter compound, while reacting with the hydrogen atom, produces CH_3 ($CH_2CO + H = CH_3 + CO$). As mentioned above, a methyl radical takes part in the reaction with C_2H_3 to form an allyl radical, a propargyl precursor, and hence a benzene precursor. Thus, in the flame of the mixture EtOH + C_2H_4, ethanol reacts, on the one hand, to form such species which later do not form PAH precursors, and, on the other hand, it contributes to the formation of PAH precursors due to, firstly, ensuring an additional pathway to form methyl radicals and, secondly, forming an additional amount of ethylene. As in the flame of the fuel mixture EtOH + C_2H_4 the fact of benzene concentration reduction has been established both experimentally and by way of computations, a conclusion can be made that the ethanol oxidation processes not resulting in PAH formation prevail, i.e., ethanol reduces the fraction of carbon forming soot precursors.

It is consistent with the previous results [7]. The reaction chain of benzene production described in the present work ($C_2H_4 \rightarrow C_2H_3 \rightarrow aC_3H_5 \rightarrow aC_3H_4 \rightarrow C_3H_3 \rightarrow C_6H_6$) is different from that presented in [7] ($C_2H_4 \rightarrow C_2H_3 \rightarrow C_2H_2 \rightarrow C_3H_3 \rightarrow C_6H_6$). This can be explained by different experimental conditions (the pressure and composition of the flames in question) and different kinetic mechanisms used. In [7], the flame with fuel equivalents ratio $\varphi = 2.34$ was studied (while in the present study $\varphi = 2.0$) at the pressure of 1 atm (while in the present study it was 30 torr), with the mechanism of Howard et al. [11] used in modeling.

5. Conclusion

The study investigates the influence of ethanol on the process of forming PAH and soot precursors in the ethylene flame by measuring and 1D kinetic modeling of the concentration profiles of stable species, as well as radicals in premixed burner-stabilized fuel-rich flame of ethylene with and without addition of ethanol at low pressure. The measurements have been made using molecular beam mass spectrometry with tunable synchrotron photoionization. Comparison of the computed and measured concentration profiles of different species has shown that the model qualitatively describes the structure of the flames under study and correctly predicts the general trend of the influence of ethanol addition on changing concentrations of intermediate products in the flame. The quantitative disagreement for some species can be explained by the fact that the mechanism used was not optimized, being composed of two mechanisms of ethylene combustion and ethanol oxidation. It has been established both experimentally and by way of modeling that the concentrations of benzene and of the propargyl radicals, the main PAH precursors, are lower in the flame with the fuel mixture ethylene/ethanol than in the ethylene flame; indicating that ethanol contributes to suppression of soot formation. The experimental reduction of propargyl concentration is significantly higher than computational, so we can assume that the mechanism of propargyl's reduction by ethanol is poorly predicted by the kinetic scheme used. Analysis of the main pathways of the reactions leading to benzene formation in the flame with ethanol and without it has shown that soot reduction in the ethylene/ethanol flame occurs due to the fact that when part of ethylene is replaced with ethanol in the initial combustible mixture, the fraction of carbon forming soot precursors decreases due to the existence of a pathway of ethanol reactions forming such species which later do not yield PAH and soot precursors.

Analysis of the main pathways of the reactions leading to benzene formation in the flame with ethanol and without it has shown that the mechanism of soot reduction consists in the fact that when part of ethylene is replaced with ethanol in the initial combustible mixture, the fraction of

carbon forming soot precursors decreases due to the existence of a pathway of ethanol reactions forming such species which later do not yield PAH and soot precursors.

Appendix A. Supplementary data

Supplementary data associated with this article can be found, in the online version, at doi:10.1016/j.proci.2010.07.066.

References

[1] F. Inal, S.M. Senkan, *Combust. Sci. Technol.* 174 (2002) 1–19.
[2] T. Kitamura, T. Ito, J. Senda, H. Fujimoto, *JSAE Rev.* 22 (2001) 139–145.
[3] K.H. Song, P. Nag, T.A. Litzinger, D.C. Haworth, *Combust. Flame* 135 (2003) 341–349.
[4] L. Xingcai, H. Zhen, Z. Wugao, L. Degang, *Combust. Sci. Technol.* 176 (2004) 1309–1329.
[5] K. Kohse-Höinghaus, P. Oßwald, U. Struckmeier, et al., *Proc. Combust. Inst.* 31 (2007) 1119–1127.
[6] K.L. McNesby, A.W. Miziolek, T. Nguyen, F.C. Delucia, R.R. Skaggs, T.A. Litzinger, *Combust. Flame* 142 (2005) 413–427.
[7] J. Wu, K.H. Song, T. Litzinger, et al., *Combust. Flame* 144 (2006) 675–687.
[8] C.S. McEnally, L.D. Pfefferle, *Proc. Combust. Inst.* 31 (2007) 603–610.
[9] B.A.V. Bennett, C.S. McEnally, L.D. Pfefferle, M.D. Smooke, M.B. Colket, *Combust. Flame* 156 (2009) 1289–1302.
[10] J. Appel, H. Bockhorn, M.Y. Frenklach, *Combust. Flame* 121 (2000) 122–136.
[11] J.B. Howard, et al., http://web.mit.edu/anish/www/MITcomb.html, (accessed October 2005).
[12] http://maeweb.ucsd.edu/~combustion/cermech/.
[13] T. Ni, S.B. Gupta, R.J. Santoro, *Proc. Combust. Inst.* 25 (1994) 585–592.
[14] T. Litzinger, M. Colket, M. Kahandawala, et al., *Combust. Sci. Technol.* 181 (2009) 310–328.
[15] M.S. Kahandawala, 2004. Ph.D. Dissertation, University of Dayton, Dayton, Ohio, 2004.
[16] S. Stouffer, R.C. Striebich, C.W. Frayne, J. Zelina, AIAA 38th Joint Propulsion Conference, 2002, p. 3723.
[17] D. Imschweiler, M. McKeand, S.-Y. Lee, et al., 39th AIAA=ASME=SAE=ASEE Joint Propulsion Conference, 2003 p. 5088.
[18] F. Qi, R. Yang, B. Yang, et al., *Rev. Sci. Instrum.* 77 (2006) 084101.
[19] J.H. Kent, *Combust. Flame* 14 (1970) 279–281.
[20] M. Kamphus, N.N. Liu, B. Atakan, F. Qi, A. McIlroy, *Proc. Combust. Inst.* 29 (2002) 2627–2633.
[21] T.A. Cool, K. Nakajima, K.A. Taatjes, et al., *Proc. Combust. Inst.* 30 (2005) 1681–1688.
[22] T.A. Cool, J. Wang, K. Nakajima, C.A. Taatjes, A. McIlroy, *Int. J. Mass Spectrom.* 247 (2005) 18–27.
[23] T.A. Cool, K. Nakajima, T.A. Mostefaoui, et al., *J. Chem. Phys.* 119 (2003) 8356–8365.
[24] J.C. Robinson, N.E. Sveum, D.M. Neumark, *J. Chem. Phys.* 119 (2003) 5311–5314.
[25] J.C. Robinson, N.E. Sveum, D.M. Neumark, *Chem. Phys. Lett.* 383 (2004) 601–605.
[26] H. Koizumi, *J. Chem. Phys.* 95 (1991) 5846–5852.
[27] Y. Li, L. Wei, Z. Tian, B. Yang, J. Wang, T. Zhang, F. Qi, *Combust. Flame* 152 (2008) 336–359.
[28] P. Desgroux, L. Gasnot, J.F. Pauwels, L.R. Sochet, *Appl. Phys. B* 61 (1995) 401–407.
[29] A.T. Hartlieb, B. Atakan, K. Kohse-Höinghaus, *Combust. Flame* 121 (2000) 610–624.
[30] H. Wang, M. Frenklach, *Combust. Flame* 110 (1997) 173–221.
[31] N.M. Marinov, *Int. J. Chem. Kinet.* 31 (1998) 183–220.
[32] N. Leplat, A. Seydi, J. Vandooren, *Combust. Sci. Technol.* 180 (2008) 519–532.
[33] A. Bhargava, P.R. Westmoreland, *Combust. Flame* 113 (3) (1998) 333–347.
[34] http://ignis.usc.edu/Mechanisms/USC-Mech%20II/USC_Mech%20II.htm.